ANL/MSD/CP-90421
CONF-961202--81

EFFECTS OF ION IMPLANTATION AND TEMPERATURE ON RADIATION-INDUCED SEGREGATION IN Ni-9Al ALLOYS*

M. J. Giacobbe[a,b], N. Q. Lam[a], P. R. Okamoto[a], N.J. Zaluzec[a], and J. F. Stubbins[b]

[a]*Materials Science Division*
9700 S. Cass Avenue
Argonne National Laboratory
Argonne, IL 60439

[b]*Department of Nuclear Engineering*
University of Illinois
Urbana, IL 61801

December 1996

Presented at the Materials Research Society 1996 Fall Meeting, Boston, MA, December 2-6, 1996.

*Work supported by the U.S. Department of Energy, Basic Energy Sciences-Materials Sciences, under contract #W-31-109-ENG-38.

DISCLAIMER

EFFECTS OF ION IMPLANTATION AND TEMPERATURE ON RADIATION-INDUCED SEGREGATION IN Ni-9Al ALLOYS

M.J. Giacobbe [1,2], N.Q. Lam [1], P.R. Okamoto [1], N.J. Zaluzec [1], and J.F. Stubbins [2]
[1] Argonne National Laboratory, Materials Science Division, Argonne, IL 60439
[2] University of Illinois at Urbana-Champaign, Dept. of Nuclear Engineering, Urbana, IL 61801

ABSTRACT

The effects of Ne and Sc implantation on radiation-induced segregation (RIS) in Ni-9at.%Al were studied in-situ utilizing the high-voltage electron microscope/Tandem accelerator facility at Argonne National Laboratory. A highly-focused 900-keV electron beam generated radial defect fluxes which, in turn, induced the transport of Al atoms toward the center of the electron-irradiated area via the inverse-Kirkendall effect. The radial segregation rate of Al atoms was monitored by measuring the diameter of the γ'-Ni_3Al zone which formed in the Al-enriched area during irradiation. Ne and Sc implantation effects on RIS were investigated at 550°C, while Ne effects were also examined at 625°C to determine the influence of temperature on the ability of Ne to act as defect trapping sites, causing RIS suppression. It was found that the RIS suppression effect of Ne increased with increasing irradiation temperature, and that Sc had a small RIS suppression effect which increased with increasing Sc implantation dose. Ne bubbles which formed during implantation are believed to be responsible for its strong suppression effect.

INTRODUCTION

Radiation-induced segregation (RIS) occurs when non uniform defect production or annihilation produces persistent defect fluxes which couple preferentially to particular alloy components [1,2]. Through two mechanisms, the inverse-Kirkendall effect and defect-solute complex migration, solute transport occurs during irradiation [1-3]. Highly-focused electron beams, which generate radial concentration gradients of point defects, have been previously used to produce RIS-induced precipitation of γ'-Ni_3Al and γ'-Ni_3Si phases in initially undersaturated Ni-Al and Ni-Si solid solutions, respectively [4-7]. The growth of these γ' phases provides a direct measure of Al or Si segregation rates during energetic electron irradiation [4-12]. Previous studies have demonstrated that Ne implantation suppresses the growth of γ'-Ni_3Al in Ni-9at.%Al irradiated with 900-keV electrons at 450 and 550°C [9,10]. In the present work, we show that this suppression effect of Ne increases with increasing temperature and that Sc implantation only provides a small suppression effect.

EXPERIMENTAL PROCEDURE

In-situ electron irradiation and ion implantation were conducted at the Argonne high-voltage electron microscope (HVEM)/Tandem accelerator facility. They were performed at 550 and 625°C with 900-keV electrons and either 75-keV Ne^+ or 200-keV Sc^+. Ne was chosen to determine the effect of temperature on its ability to mitigate RIS, while Sc, which has demonstrated strong binding with vacancies in rapidly quenched Cu [11], was selected to study its effect on segregation kinetics. TRIM calculations show that 100% of the 75-keV Ne^+ ions and 99% of the 200-keV Sc^+ ions are stopped within a distance of 180 nm from the top foil surface.

A focused electron beam produces a non uniform defect distribution in a thin film as shown in Figure 1. The effective beam diameter of the focused beam, D_o, is defined by $I_T = I_o(\pi D_o/2)^2$, where I_T is the total electron current and I_o is the maximum electron flux. When the beam is Gaussian in nature, $D_o=2\sqrt{2}\sigma$, where σ is the standard deviation of the beam intensity profile. During irradiation of Ni-Al alloys, Al atoms migrate against the induced vacancy flux, and the section of the irradiated zone in which the defect concentration profile is concave downward becomes enriched with Al [7,8]. Al enrichment continues in the irradiated area until its solubility limit is reached, at which point the γ'-Ni_3Al phase nucleates and grows [4,5]. The growth of the precipitate zone thus provides a direct measure of the Al radial segregation rate.

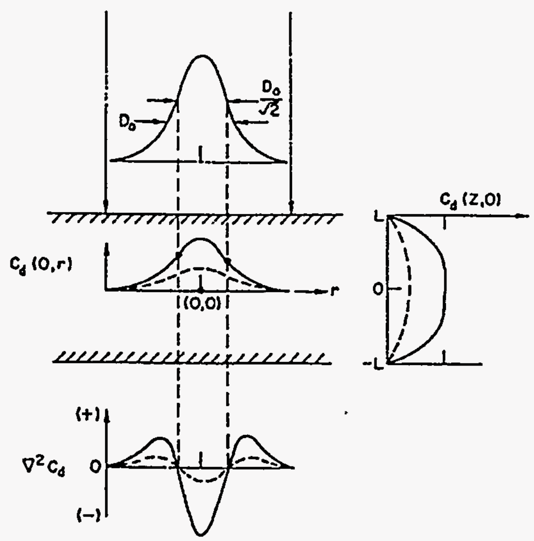

Figure 1. Top to bottom: electron beam profile, radial and axial defect concentration profiles, and radial defect divergence. The defect gradients determine the direction and magnitude of the defect flux, while the defect divergence determines the local rate of solute accumulation or depletion [7,8].

In the present investigation, peak electron damage rates varied between 5.4 - 8.4×10^{-4} dpa/s. Two types of irradiations were performed: (i) electrons only and (ii) ion implantation followed by electron irradiation. γ'-Ni_3Al precipitate zones were pre-formed by electron irradiation during (ii) to act as reference markers. In one case, however, the sample was ion irradiated with 2×10^{16} Sc/cm^2 before the irradiation zone was subject to any high energy electrons. During the Sc experiments, the shapes of the focused electron beam and the resultant precipitate zone were circular, while during the Ne experiments they were elliptical. The diameter of the circular beams ranged from 1 - 1.1 μm in diameter, whereas the size for elliptical beams ranged from 1.1 - 1.3 μm on the major axis and from 0.91 - 1.1 μm on the minor axis. The beam was assumed to be Gaussian in the circular case and bi-Gaussian in the elliptical case. Hence, their intensities were assumed to be $I(r) = I_o\exp(-r/r_o)^2$ and $I(x,y) = I_o\exp\{-(x/a_o)^2 - (y/b_o)^2)\}$, respectively, where $r_o = \sqrt{2}\sigma$, $a_o = \sqrt{2}\sigma_a$, and $b_o = \sqrt{2}\sigma_b$ with σ being the standard deviation for the circular beam condition, and σ_a and σ_b being the standard deviations along the major and minor axes for the elliptical beam condition. The dimensions of the precipitate zones were measured as ratios of precipitate zone size over $\sqrt{2}\sigma$, i.e. d/d_o or a/a_o and b/b_o, and this ratio allows for measurements to be normalized for varying electron beam conditions. Therefore, results can be presented on the same scale.

RESULTS

The results are summarized in Figs. 2 - 6. Figure 2 shows the γ'-Ni_3Al precipitate growth under electron only and Sc implanted-electron irradiation conditions. In the Sc implantation case, a γ' zone was seeded, or pre-formed by 900-keV electron irradiation before any Sc bombardment, as seen in Fig. 3b showing the seeded zone after 0.47 dpa. The same method was applied to the Ne implantation experiments seen in Figs. 4b - c, where precipitate zones were seeded to 0.60 and

0.49 dpa at 550 and 625°C, respectively. In each Ne case, 550 and 625°C, an electron only standard run was performed, but only the 550°C standard is shown in Fig. 4a.

Figures 2 and 3b demonstrate the effects of Sc implantation on RIS. After $2x10^{15}$ Sc/cm^2, the Ni_3Al growth was slightly mitigated as supported by the micrographs in Fig. 3b. A subsequent experiment where Sc implantation to $2x10^{16}$ Sc/cm^2 preceded any electron irradiation showed a greater suppression effect. The effects of Ne implantation on Al segregation at 550 and 625°C can be seen in Figs. 4a - c. Increasing irradiation temperature greatly increased the Ne suppression effect.

This trend is better illustrated in Fig. 5, which shows the suppression effect of both Ne and Sc expressed as the suppression fraction. The suppression fraction curves are calculated as the difference in standard and post-implantation γ'-Ni_3Al precipitate growth curves divided by the standard precipitate growth curve. At 550°C, the suppression fraction curve for Sc lies below 0.1, indicating it has a very small effect in quelling Al transport to the electron irradiated area. Not shown in Fig. 5 is the suppression fraction curve resulting from implantation of $2x10^{16}$ Sc/cm^2 at 550°C because only the final data point was obtained from the γ'-Ni_3Al growth curve. The supression fraction value at the final point was 0.15, or about twice that from the $2x10^{15}$ Sc/cm^2 case. From Fig. 2 it appears the value of 0.15 is too small, but unlike all other values in Fig. 5, it was calculated from the inital point of the electron standard run. At 625°C, RIS is completely shut down after implantation of $1.31x10^{15}$ Ne/cm^2. The total suppression of RIS is attributed to the formation of Ne bubbles (Fig. 6), which act as vacancy trapping sites, hence reducing the number of defects free to participate in RIS.

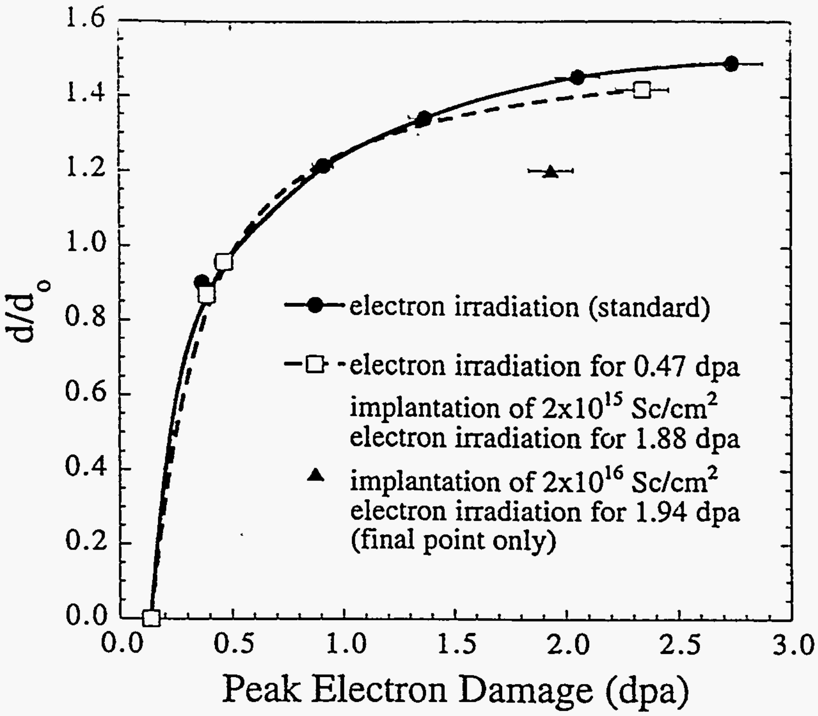

Figure 2. γ'-Ni_3Al growth curve for 900-keV electron standard irradiation, 900-keV electron irradiation which followed precipitate seeding and implantation of $2x10^{15}$ Sc/cm^2, and 900-keV electron irradiation which followed implanation of $2x10^{16}$ Sc/cm^2 at 550°C. Plotted on the y-axis is the ratio of the precipitate zone size to the Gaussian beam dimensions, which allows for the normalization of irradiations with varying electron beam conditions.

An interesting feature first reported in [9], is the sink-denuded zone (Fig. 4b) surrounding the γ'-Ni_3Al precipitate which formed after Ne implantation at 550°C. Also, no visible sink structure was found around the precipitate zone after implantation at 625°C. Sc implantation to $2x10^{15}$ ions/cm^2 at 550°C, on the other hand, produces a complex dislocation network, which required the precipitate zone to be imaged with a superlattice spot in order to be separated from the induced damage background.

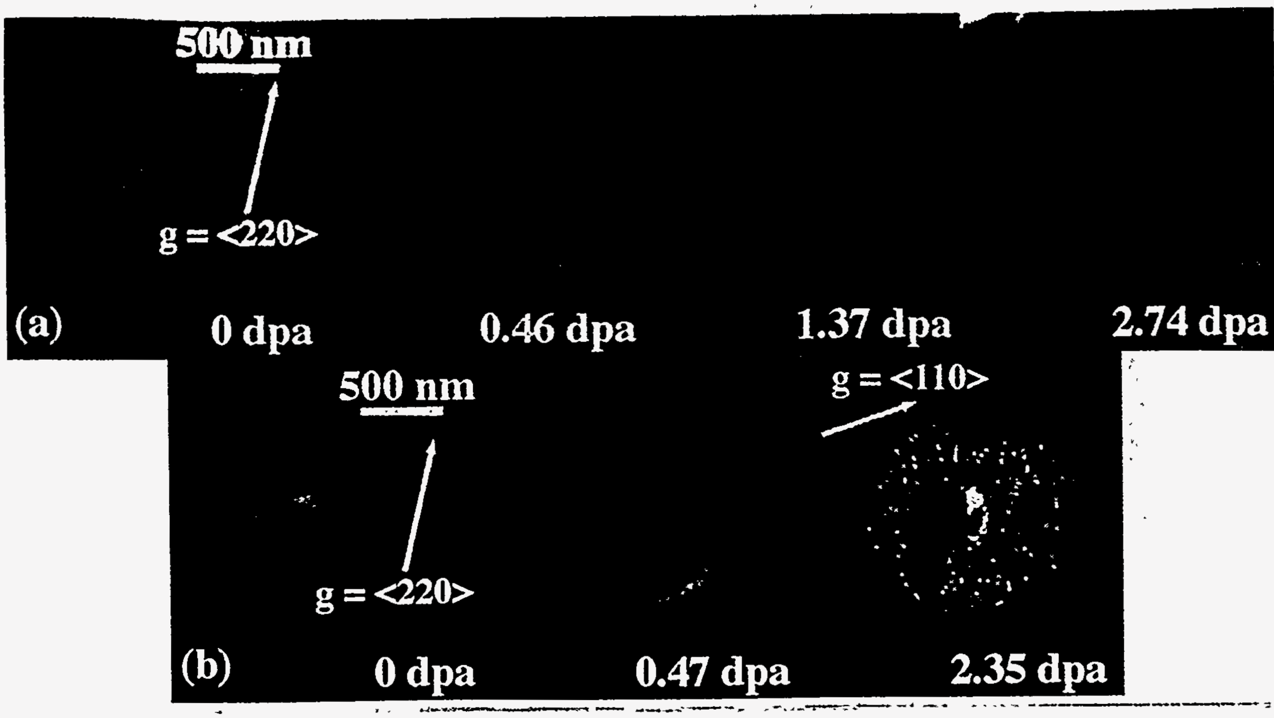

Figure 3. Ni_3Al precipitate growth as a function of peak electron dose for (a) 900-keV electron irradiation to 2.74 dpa, and (b) 900-keV electron irradiation to 0.47 dpa to seed a precipitate zone, followed by implantation of 2×10^{15} Sc/cm^2 and subsequent 900-keV electron irradiation for 1.88 dpa to a total of 2.35 dpa. Both irradiations were performed at 550°C.

DISCUSSION

Our study demonstrates that increasing irradiation temperature from 550 to 625°C dramatically increases the suppression effect of Ne on RIS. The results also show that the effect of Sc implantation is rather small and seems to increase with increasing dose. The effects cannot be attributed to a change in the visible sink structure incurred during ion implantation as previously shown during Ni implantation in Ni-9at.%Al at 550°C [10]. Increasing Sc implantation dose resulted in increased suppression, which is consistent, although not as dramatic, with the trend found for Ne implantation in Ni-9at.%Al at 450°C [9].

Since atom transport by RIS is driven by defects that survive annihilation and recombination, the results presented here suggest that Ne acts as strong vacancy trapping sites, hence reducing the out-flux of vacancies from the electron beam center. In fact, micrographs of Ne implanted Ni-9at.%Al at 625°C show evidence of Ne bubble formation which, similar to He clusters in Ni-based alloys [12], act as strong trapping sites, reducing segregation.

The effect of Sc implantation on segregation kinetics is not completely understood, and further studies are necessary to determine its role in RIS suppression. Experiments involving Ne implantation to 10^{15} Ne/cm^2 are also necessary at other temperatures to better understand the influence of temperature on RIS.

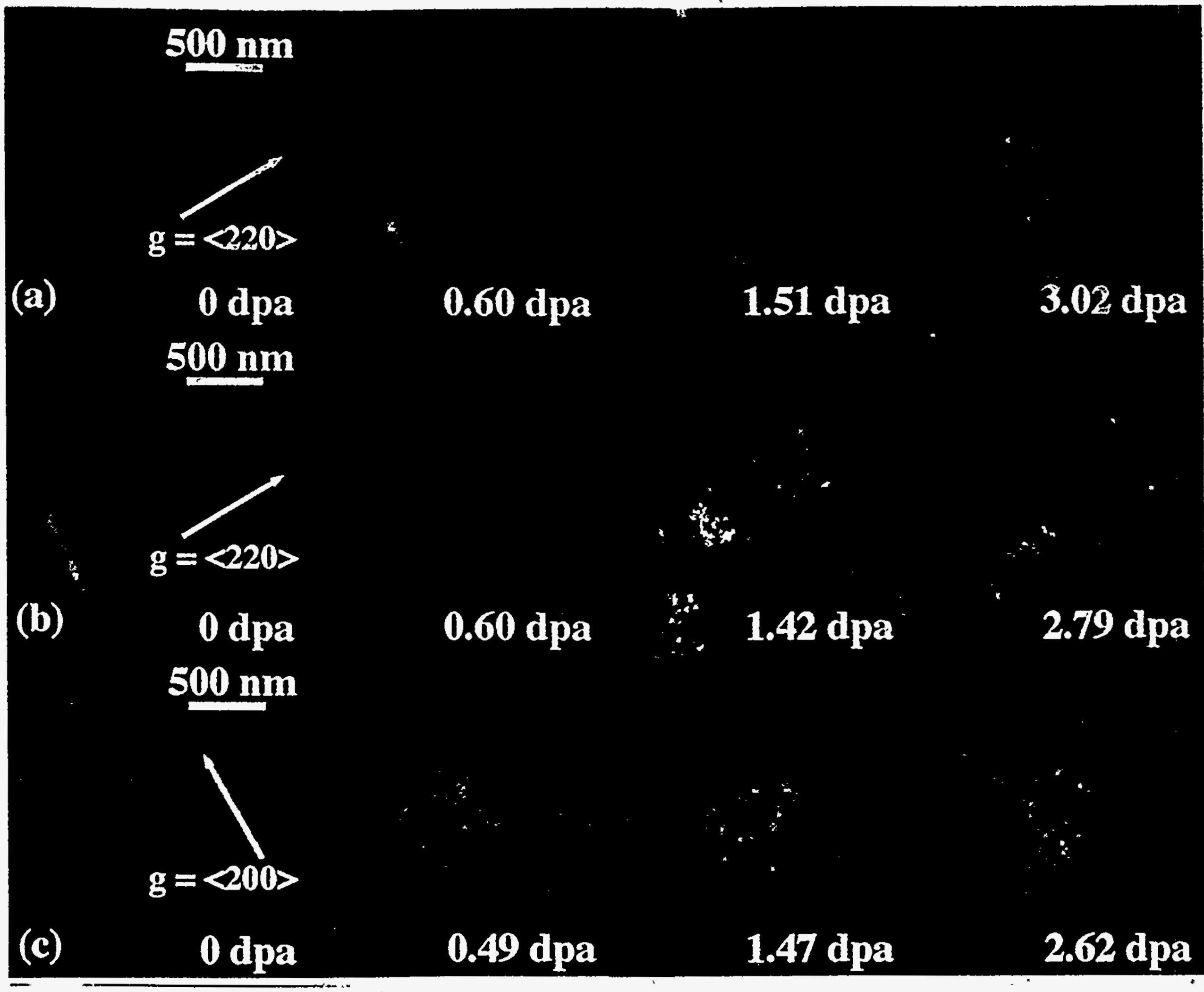

Figure 4. Ni_3Al precipitate growth as a function of peak electron dose for (a) 900-keV electron irradiation, (b) 900-keV electron irradiation to 0.60 dpa to seed a precipitate zone, followed by implantation of 10^{15} Ne/cm^2 and subsequent 900-keV electron irradiation for 2.19 dpa to a total of 2.79 dpa, and (c) 900-keV electron irradiation to 0.49 dpa to seed a precipitate zone, followed by implantation of 1.31×10^{15} Ne/cm^2 and subsequent 900-keV electron irradiation for 2.13 dpa to a total of 2.62 dpa. Irradiations (a) and (b) were performed at 550°C, and (c) was performed at 625°C

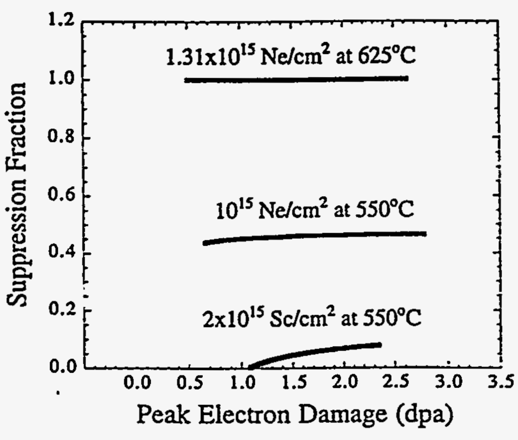

Figure 5. RIS suppression fraction as a function of peak electron damage for Ne at 550 and 625°C and for Sc at 550°C. A value of 0 indicates no suppression effect from the implantation, while a value of 1 indicates complete suppression.

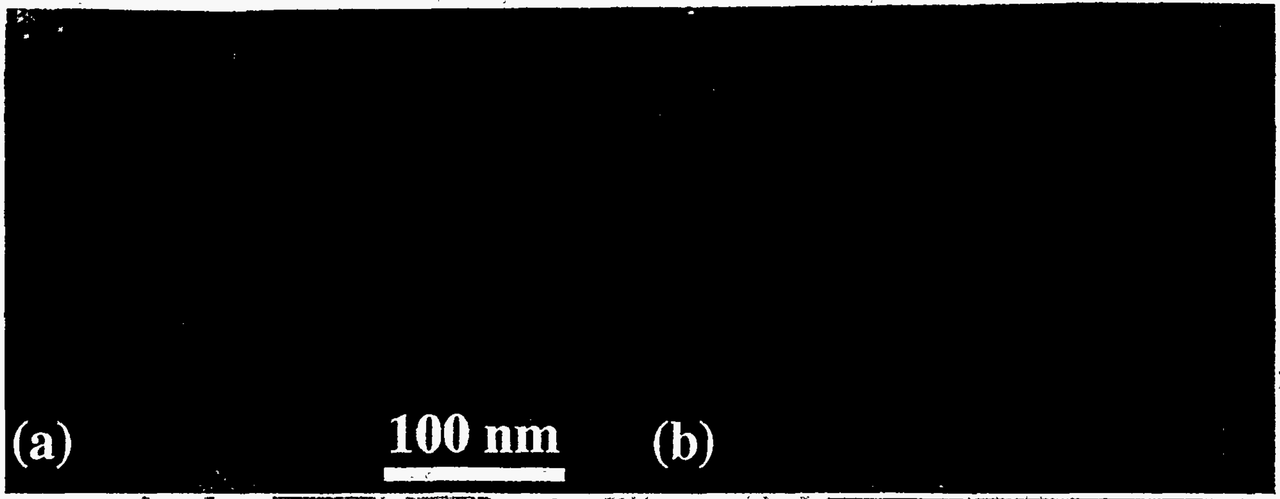

Figure 6. (a) Underfocused and (b) overfocused images of Ni-9at.%Al implanted with 4.2×10^{15} Ne/cm^2. White spots in the underfocused and corresponding dark spots in the overfocused conditions are a strong indication of Ne bubble formation.

CONCLUSION

Ne implantation to ~10^{15} Ne/cm^2 in Ni-9at.%Al irradiated with 900-keV electrons at 550 and 625°C shows a strong suppression effect on RIS, which increases with increasing temperature. Sc implantation up to 2×10^{16} Sc/cm^2 demonstrated that Sc has only a small effect on segregation kinetics at 550°C and is not as effective as Ne in mitigating Al segregation.

ACKNOWLEDGMENTS

The authors would like to thank R.C. Birtcher and L.E. Rehn for helpful discussions They are also grateful to B. Kestel, E. Ryan. S. Ockers, and L. Funk for their experimental assistance.

REFERENCES

[1] P.R. Okamoto and L.E. Rehn, J. Nucl. Mater. **83** , 2(1979).
[2] H. Wiedersich and N.Q. Lam, in: *Phase Transformations during Irradiation*, ed. F.V. Nolfi, Jr. (Applied Science Publishers, London, 1983) p. 1.
[3] R.A. Johnson and N.Q. Lam, Phys. Rev **B13**, 4364 (1976).
[4] N.Q. Lam, G.K. Leaf, and M. Minkoff, J. Nucl. Mater. **118**, 248 (1983).
[5] N.Q. Lam and P.R. Okamoto, in *Effect of Radiation on Materials: Twelfth International Symposium*, ASTM STP 870, eds. F.A. Garner and J.S. Perrin (ASTM, Philadelphia 1985) p. 430.
[6] N.Q. Lam and P.R. Okamoto, J. Nucl. Mater. **133-134**, 430 (1985).
[7] N.Q. Lam and P.R. Okamoto in *Solute-Defect Interaction: Theory and Experiment*, eds. S. Saimoto et al. (Pergamon Press, Toronto, 1986) p. 307.
[8] P.R. Okamoto and N.Q. Lam, Mat. Res. Soc. Symp. Proc. **41**, 241 (1985): N.Q. Lam, P.R. Okamoto, and G.K. Leaf, Mat. Res. Soc. Symp. Proc. **74**, 523 (1987).
[4] N.Q. Lam, G.K. Leaf, and M. Minkoff, J. Nucl. Mater. **118**, 248 (1983).
[9] M.J. Giacobbe, N.Q. Lam, P.R. Okamoto, N.J. Zaluzec, and J.F. Stubbins, MSA Proc., 988 (1996).
[10] M.J. Giacobbe, N.Q. Lam, P.R. Okamoto, and J.F. Stubbins, Mat. Res. Soc. Symp. Proc. **396**, 57 (1995).
[11] A.S. Berger and R.W. Siegel, J. Phys. F: Metal Phys., **9**, L67 (1979).
[12] T. Ezawa, E. Wakai, T. Tanabe, and R. Oshima, J. Nucl. Mater. **191-194,** 1346 (1992).